INTERNATIONAL JOURNAL FOR NUMERICAL METHODS IN FLUIDS, VOL. 8, 965–975 (1988)

TWO-EQUATION (k, ε) TURBULENCE COMPUTATIONS BY THE USE OF A FINITE ELEMENT MODEL

TORBJØRN UTNES

Norwegian Hydrotechnical Laboratory, N-7034 Trondheim-NTH, Norway

SUMMARY

A finite element technique is presented and applied to some one- and two-dimensional turbulent flow problems. The basic equations are the Reynolds averaged momentum equations in conjunction with a two-equation (k, ε) turbulence model. The equations are written in time-dependent form and stationary problems are solved by a time iteration procedure. The advection parts of the equations are treated by the use of a method of characteristics, while the continuity requirement is satisfied by a penalty function approach. The general numerical formulation is based on Galerkin's method. Computational results are presented for one-dimensional steady-state and oscillatory channel flow problems and for steady-state flow over a two-dimensional backward-facing step.

KEY WORDS Finite element method Turbulent flow Method of characteristics Penalty function approach Galerkin method

INTRODUCTION

Finite element methods are well established in the field of structural mechanics and their applications to fluid mechanics seem to be increasing, although finite difference methods still dominate most of this field at present. This is especially the case for the computation of high-Reynolds-number flows and turbulent flows.[1]

However, several finite element papers have been published on turbulent flow problems during the last few years (see e.g. References 2–11). As in the case of finite difference methods, much of this work has been related to the solution of the so-called (k, ε) turbulence model in conjunction with the Reynolds averaged momentum equations. In addition, many of these finite element studies have concentrated on the solution of the steady-state form of these equations.

Alternatively, one can solve the equations in time-dependent evolutionary form, even for steady-state problems. This approach is of course necessary if the aim is to solve problems with time-dependent boundary conditions. The present paper presents a finite element method based on this approach. The characteristics method is introduced to obtain a stable and accurate computation of the advection for both the momentum and the (k, ε) equations. This procedure results in a symmetric coefficient matrix for the remaining equation system. The source terms in the (k, ε) model are treated in a similar fashion to a commonly used finite difference technique, and the velocity, kinetic energy and dissipation are interpolated bilinearly over each element. Computational results are presented for some 'standard' problems, indicating realistic solutions in these cases.

0271–2091/88/080965–11$05.50

Received 20 July 1987
Revised 24 November 1987

MATHEMATICAL FORMULATION

The Reynolds averaged momentum and continuity equations for incompressible turbulent flow without gravity are given by

$$(\rho U_i)_{,t}+(\rho U_i U_j)_{,j}=-P_{,i}+(\tau_{ij}-\rho\overline{u_i u_j})_{,j}, \tag{1}$$

$$U_{i,j}=0. \tag{2}$$

Where U_i is the mean velocity, ρ is the fluid density, P is the mean pressure and τ_{ij} is the mean viscous stress tensor defined by

$$\tau_{ij}=\mu(U_{i,j}+U_{j,i}), \tag{3}$$

where μ is the molecular viscosity. Differentiation with respect to x_i or t is indicated with a comma followed by 'i' or 't' and Einstein's summation convention is used. By employing the Boussinesq assumption, the Reynolds stress for incompressible flow can be written as

$$-\rho\overline{u_i u_j}=\mu_t(U_{i,j}+U_{j,i})-\tfrac{2}{3}\rho k\delta_{ij}, \tag{4}$$

where μ_t is a turbulent viscosity coefficient, δ_{ij} is the Kronecker delta and k is the mean turbulent kinetic energy,

$$k=\overline{u_i u_i}/2. \tag{5}$$

By redefining the pressure as

$$P^*=P+\tfrac{2}{3}\rho k, \tag{6}$$

the following modification of equation (1) is derived:

$$(\rho U_i)_{,t}+(\rho U_j U_i)_{,j}=-P^*_{,i}+[\mu_e(U_{i,j}+U_{j,i})]_{,j}, \tag{7}$$

where $\mu_e=\mu_t+\mu$ is denoted the 'effective' viscosity.

In order to solve the dynamical equations (2) and (7), the turbulent viscosity must be specified. Here the two-equation (k, ε) turbulence model is used for that purpose, in which μ_t is given by

$$\mu_t=\rho C_\mu k^2/\varepsilon, \tag{8}$$

where C_μ is assumed to be a constant and ε is the rate of dissipation of k. The transport equations for k and ε are[12]

$$(\rho k)_{,t}+\rho U_j k_{,j}=[(\mu+\mu_t/\sigma_k)k_{,j}]_{,j}+\mu_t S_u-\rho\varepsilon, \tag{9}$$

$$(\rho\varepsilon)_{,t}+\rho U_j\varepsilon_{,j}=[(\mu+\mu_t/\sigma_\varepsilon)\varepsilon_{,j}]_{,j}+C_1 C_\mu\rho k S_u-C_2\varepsilon^2/k, \tag{10}$$

where the source term S_u is given by

$$S_u=U_{i,j}(U_{i,j}+U_{j,i}) \tag{11}$$

and the model constants are assumed to have their 'conventional' values:[12]

$$(C_\mu, C_1, C_2, \sigma_k, \sigma_\varepsilon)=(0{\cdot}09, 1{\cdot}44, 1{\cdot}92, 1{\cdot}0, 1{\cdot}3). \tag{12}$$

In order to solve the complete equation system (2), (7)–(11), initial and boundary conditions must be specified. The boundary conditions applied are as follows.

Inflow boundaries

Specified Dirichlet conditions for all the variables (U_i, k, ε).

Free boundaries

Traction-free velocity–pressure condition:

$$-P^*_{,i}+\mu_e(U_{i,j}+U_{j,i})=0. \tag{13}$$

Zero normal derivative of (k, ε):

$$\partial k/\partial n=\partial\varepsilon/\partial n=0. \tag{14}$$

Wall boundaries

Logarithmic near-wall conditions:

$$U_\tau=U_* \ln(h^+)/\kappa, \tag{15}$$

where $h^+=9hU_*/\nu$ for smooth walls and $h^+=30h/K_s$ for rough walls;

$$k=U_*^2/C_\mu^{1/2}, \qquad \varepsilon=U_*^3/kh. \tag{16}$$

Here U_τ is the velocity component tangential to the wall, U_* is the friction velocity, ν is the kinematic viscosity, κ is the von Karman constant, K_s is a roughness parameter and h is a small distance from the wall specified by $hU_*/\nu>30$ for smooth walls. For smaller values the condition for U_τ must be modified. However, in that case the present (k, ε) model should also be generalized.[13]

An alternative condition for k has also been used,[8] namely, assuming a constant k region near the wall, implying that $\partial k/\mathrm{d}n=0$. With this condition the ε condition in (16) can be written in the equivalent form

$$\varepsilon=C_\mu^{3/4}k^{3/2}/kh.$$

A wall boundary condition must also be specified for the normal component of the velocity. Here we have used the form $U_n=0$, but a more accurate condition is available.[5]

NUMERICAL METHOD

Equations (7), (9) and (10) can all be classified as advection–diffusion equations and may be written as

$$f_{,t}+U_j f_{,j}=s, \tag{17}$$

with only the advection operator written out explicitly. Let the characteristics directions associated with this operator be $T=T(\mathbf{x})$ and the corresponding characteristics $\mathbf{X}(\mathbf{x}, t; T)$. When $\mathbf{U}$ is the velocity field of the fluid, then $\mathbf{X}(\mathbf{x}, t; T)$ represents the particle path that passes through $\mathbf{x}$ at time t. These characteristics are determined from the following ordinary differential equation:

$$\mathrm{d}\mathbf{X}/\mathrm{d}T=\mathbf{U}(\mathbf{X}, T), \tag{18}$$

with the initial condition

$$\mathbf{X}(T=t)=\mathbf{x}.$$

Along these characteristics equation (17) is transformed to

$$df(\mathbf{X}, T)/dT|_{T=t} = s. \tag{19}$$

A semi-implicit discretization of (19) gives

$$[f(\mathbf{X}^{n+1}) - f(\mathbf{X}^n)]/\Delta t = (1-\alpha)s^{n+1} + \alpha s^n, \qquad \alpha \in [0, 1], \tag{20}$$

where $\mathbf{X}^{n+1}$ coincides with $(\mathbf{x}, t^{n+1})$ and $\mathbf{X}^n$ must be determined from (18). The numerical computation of $\mathbf{X}^n$ was performed by the use of a second-order Runge–Kutta method on the velocity field at time t^n. This application of the characteristics method in a finite element context has been studied by several authors[14–18] and has some appealing properties: the numerical stability is good, no upwinding technique is necessary and the resulting equation system becomes symmetric. On the other hand it is not straightforward to implement such a method efficiently.

A formulation corresponding to (20) is now applied to all the governing equations ((7), (9) and (10)), which are multiplied by a weighting function, integrated over the computational domain and subsequently discretized by the use of a standard Galerkin finite element method. A penalty approximation is applied to satisfy the continuity equation[19,20] and, following a conventional procedure, the discretized equations can finally be written in the following form:

$$\{\mathbf{M}/\Delta t + (1-\alpha)[\mathbf{D} + r\mathbf{C}\mathbf{L}^{-1}\mathbf{C}^T]\}\mathbf{U}^{n+1} = (\mathbf{M}/\Delta t)\mathbf{U}^n(\mathbf{X}^n) + (1-\alpha)\mathbf{F}^{n+1} + \alpha\mathbf{F}^n - \alpha(\mathbf{D} + r\mathbf{C}\mathbf{L}^{-1}\mathbf{C}^T)\mathbf{U}^n - \alpha\mathbf{C}\mathbf{P}^{n+1}, \tag{21}$$

$$\mathbf{P}^{n+1} = r\mathbf{L}^{-1}\mathbf{C}^T\mathbf{U}^{n+1}. \tag{22}$$

Here $(\mathbf{U}, \mathbf{P})$ denote the global velocity and pressure vectors, $\mathbf{M}$ is the velocity mass matrix, $\mathbf{D}$ is the diffusion matrix, $\mathbf{C}$ is the divergence matrix, $\mathbf{L}$ is the pressure mass matrix and $\mathbf{F}$ is a vector containing boundary condition contributions. The parameter r is the penalty parameter and α controls the implicitness of the formulation. Because of the large value of r, which is necessary to satisfy the continuity condition, it is important to keep the system A-stable; hence α should be chosen between 0 and $\frac{1}{2}$. In these equations the index 'n' denotes the time step and 't' the matrix transpose. In the computations the following space discretization was used: quadrilateral elements with bilinear interpolation of the velocity field and constant (discontinuous) approximation of the pressure.

The total coefficient matrix on the left side in (21) is symmetric, but variable in time. A more efficient way to solve this system is to split the diffusion matrix according to

$$\mathbf{D}(\mu_e) = \mathbf{D}(\mu_0) + \mathbf{D}(\mu_e - \mu_0), \tag{23}$$

where μ_0 is the turbulent viscosity at some previous time. The part $\mathbf{D}(\mu_0)$ is kept on the left side in (21), while the residual part is treated explicitly. This splitting replaces the α-splitting of the diffusion matrix in (21) and makes a matrix factorization necessary only each time μ_0 is updated.

The corresponding discretized form of the (k, ε) equations can be written as follows:

$$\{\mathbf{M}/\Delta t + (1-\alpha)\mathbf{D}_k\}\mathbf{K}^{n+1} = (\mathbf{M}/\Delta t)\mathbf{K}^n(\mathbf{X}^n) + (1-\alpha)\mathbf{F}_k^{n+1} + \alpha\mathbf{F}_k^n + (1-\alpha)\mathbf{S}_k^{n+1} + \alpha(\mathbf{S}_k^n - \mathbf{D}_k\mathbf{K}^n), \tag{24}$$

$$\{\mathbf{M}/\Delta t + (1-\alpha)\mathbf{D}_\varepsilon\}\mathbf{E}^{n+1} = (\mathbf{M}/\Delta t)\mathbf{E}^n(\mathbf{X}^n) + (1-\alpha)\mathbf{F}_\varepsilon^{n+1} + \alpha\mathbf{F}_\varepsilon^n + (1-\alpha)\mathbf{S}_\varepsilon^{n+1} + \alpha(\mathbf{S}_\varepsilon^n - \mathbf{D}_\varepsilon\mathbf{E}^n). \tag{25}$$

In these equations $(\mathbf{K}, \mathbf{E})$ represent the nodal vectors of (k, ε), $\mathbf{M}$ is the mass matrix, $\mathbf{D}$ is the combined diffusion and dissipation matrix, $\mathbf{S}$ is the source vector and $\mathbf{F}$ is the boundary value

vector. It should be noted that the advection parts of these equations are treated by the use of the method of characteristics, in a similar way to the momentum equations. The space discretization of the k and ε fields is done by bilinear interpolation in both cases. The source quantities are also written in bilinear form, interpolated from averaged nodal values of the velocity derivatives, and the dissipation terms are linearized in a way commonly used in finite difference codes.[21] The diffusion and dissipation terms are here collected in the **D**-matrices in (24) and (25). Finally, the turbulent viscosity is computed by application of (8) to the nodal values and bilinearly interpolated over each element.

The implementation of boundary conditions in these equations is quite conventional, except possibly for the velocity–pressure log condition. This condition was implemented via a 'stress boundary' formulation,[22] where the stress integral which follows naturally from the Galerkin formulation of the momentum equations was used. If the velocity at the boundary is decomposed into components normal and tangential to the wall, the tangential component of the stress integral takes the form

$$F_\tau = \int_\Gamma W(\partial U_\tau/\partial n + \partial U_n/\partial \tau)\mu_e \, d\Gamma, \tag{26}$$

where W is the weighting function and the integral is over the wall boundary Γ. The log condition is now implemented directly via the normal derivative of the tangential velocity in (26).

The complete (**U**, **P**, **K**, **E**) system is solved by a decoupling of the (**U**, **P**) and (**K**, **E**) systems. The velocity–pressure equations are solved from (21) and (22) with a known turbulent viscosity from previous computations of the (k, ε) fields, while the turbulence model is solved from (24) and (25) with previous values of the velocity and viscosity fields. Although the equation system is strongly coupled and non-linear, this decoupling procedure was found to work well for all the test cases presented here. For stationary problems the time integration acts as an iteration process. However, an iteration procedure should formally be applied between each time step when the boundary conditions are time-dependent. Numerical experiments with the 1D time-dependent problem studied here, however, showed that more important stability constraints are attributed to the implementation of the wall boundary condition (26). Initially this condition was written in explicit form, but was later modified to a semi-implicit formulation, which improved the stability range substantially.

APPLICATIONS TO TURBULENT FLOW PROBLEMS

The computational results presented here were all performed with $\alpha = 0$, i.e. a fully implicit formulation, except for the splitting of the diffusion matrix in (23), where an updating procedure was implemented to keep the equation system absolutely stable.

The first test case is for a 1D steady-state channel flow problem with boundary conditions as shown in Figure 1 and with a computational grid consisting of 14 graded elements. The Reynolds number based on the channel depth is $Re_h = 60000$. Results are shown in Figures 2 and 3 for velocity and turbulent kinetic energy profiles. It is seen that the predicted velocity profile is in good agreement with experimental results,[23] but the k level is not very accurately predicted. On the other hand the present computations are in close agreement with other numerical results based on the same turbulence model[2] and improvements of the k predictions for this test can probably be obtained by modifications of the model constants.

The same grid as above was used for the computation of a harmonic oscillating channel flow, where a sinusoidal pressure gradient with period $T = 8.39$ s was imposed. Here the kinematic

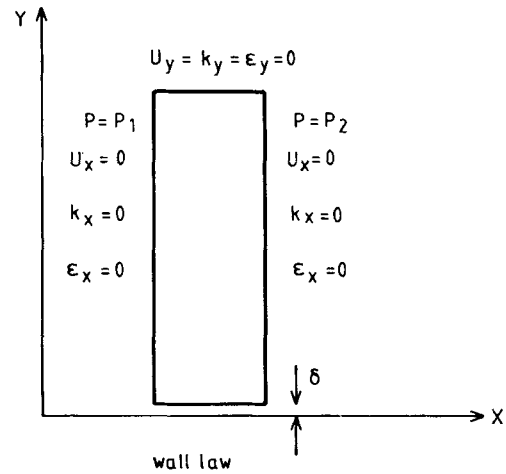

Figure 1. Geometry and boundary conditions for 1D channel flow

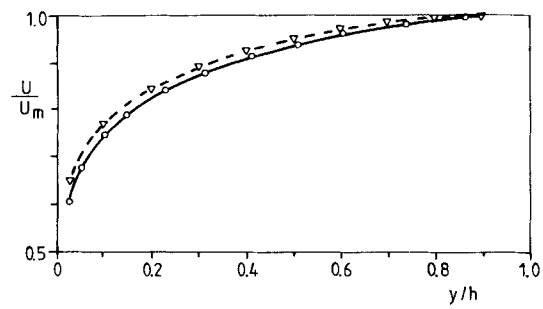

Figure 2. Velocity profile for 1D steady-state channel flow: —o—, present computation; – –▽– –, Laufer[23]

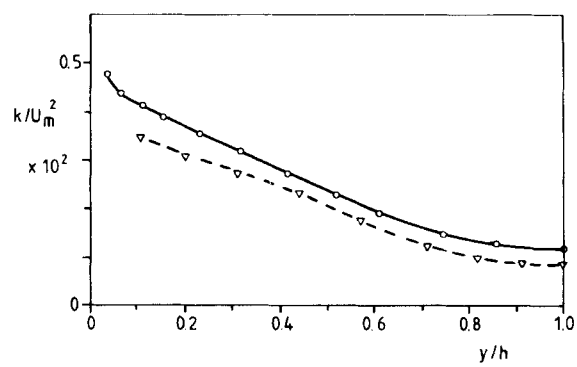

Figure 3. Kinetic energy for 1D steady-state channel flow: —o—, present computation; – –▽– –, Laufer[23]

viscosity $\nu = 10^{-6}$ and the bottom surface is rough, with a roughness parameter $K_s = 2.3$ cm. Experimental results for this problem are given by Jonsson and Carlsen.[24] The present computations were performed with a time step $\Delta t = T/160$, which was found to give a satisfactory 'convergent' solution, i.e. smaller time steps did not have much influence on the solution. No iterations were performed in these calculations and a time step limit is therefore necessary also for stability reasons. In order to reach a periodic solution, the computations were run for about three cycles. Results of velocity profiles at different phases are shown in Figure 4 compared with measurements. Similar results for the maximum shear stress are shown in Figure 5. The agreement is relatively good for the velocity profiles, while the predicted shear stress amplitude is somewhat small. The model constants can again be tuned to give better agreement compared with measurements, but this was not seriously considered here. It should be noted that the shear stress was estimated indirectly in Reference 24, by a vertical integration of the momentum equation, and this could also imply some inaccuracy.

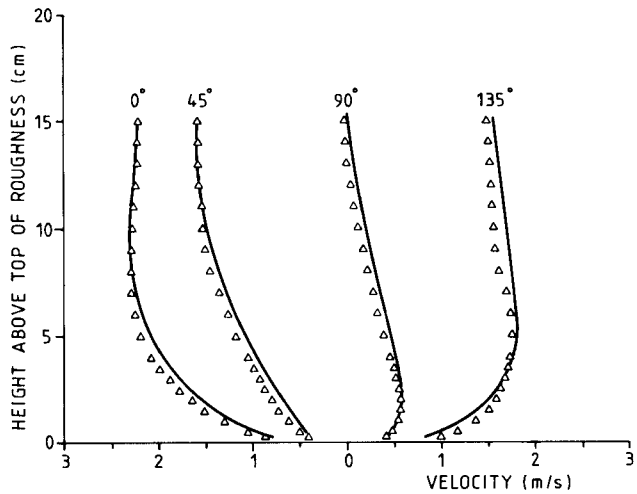

Figure 4. Velocity profiles for 1D oscillating channel flow: ——; present computation; △, Jonsson and Carlsen[24]

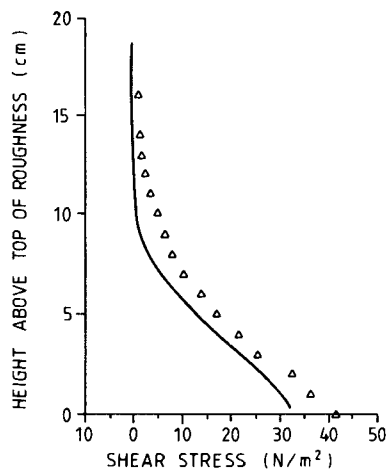

Figure 5. Maximum shear stress for 1D oscillating channel flow: ——, present computation; △, Jonsson and Carlsen[24]

The third test case concerns the turbulent flow over a backward-facing step, previously reported by several authors.[2,5,10] Experimental results are given by Westphal *et al.*[25] among others. The present computations were performed for a Reynolds number $Re_h = 42000$ based on the step height h. The geometry is shown in Figure 6 together with the applied boundary conditions, the ratio $H/h = \frac{3}{2}$, where H is the inflow channel height, and the computational grid consists of 21×18 graded elements with the outflow boundary situated a distance $17h$ downstream from the step. The simulation was initiated from the Stokes solution of a laminar flow field. Comparisons of numerical and experimental results are shown in Figures 7 and 8 for sections located at $x/h = 4, 8, 12$. It is seen that the velocity profile prediction is relatively good in the recirculation zone, although the k level is less accurate. Downstream of the reattachment point the predicted velocity is less accurate and recovers more slowly to a quasi-1D profile than indicated by the measurements. The reattachment point is here computed at approximately $x_R = 8{\cdot}6$, which is somewhat large compared with the measured value of about 7·3–7·5.[25,26] It may be interesting to note that this result is contrary to other computations, where x_R becomes too small.[11,27] However, the same tendency of too slow recovery downstream of x_R is observed. It has

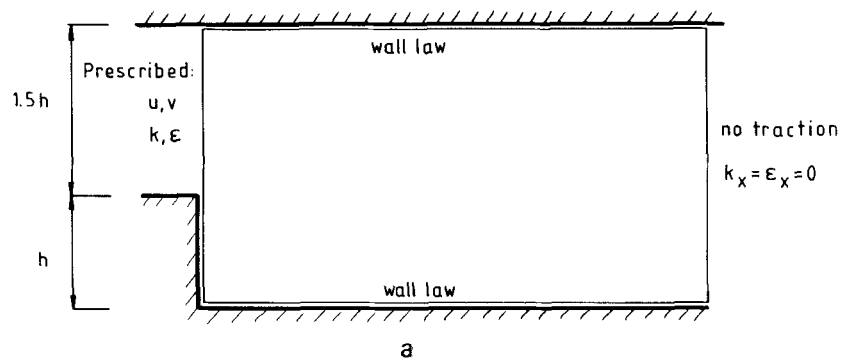

Figure 6(a). Geometry and boundary conditions for backward-facing step

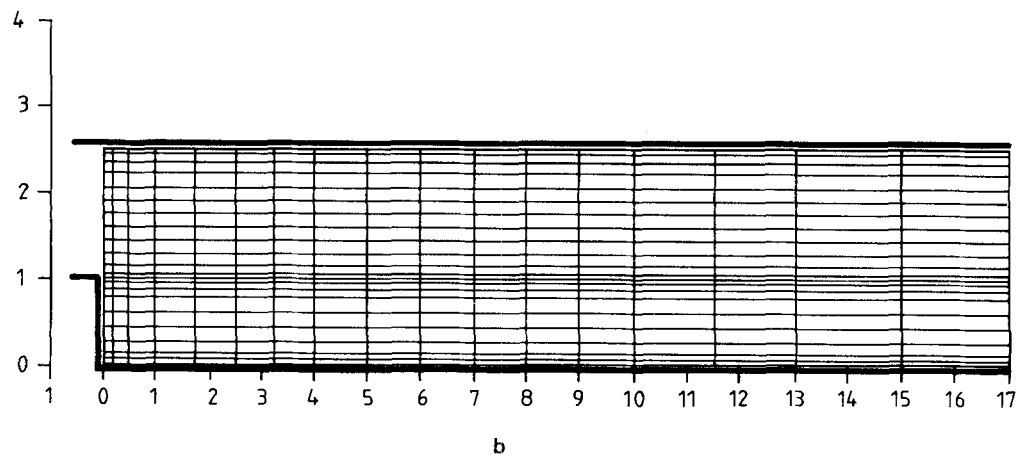

Figure 6(b). Finite element grid for backward-facing step

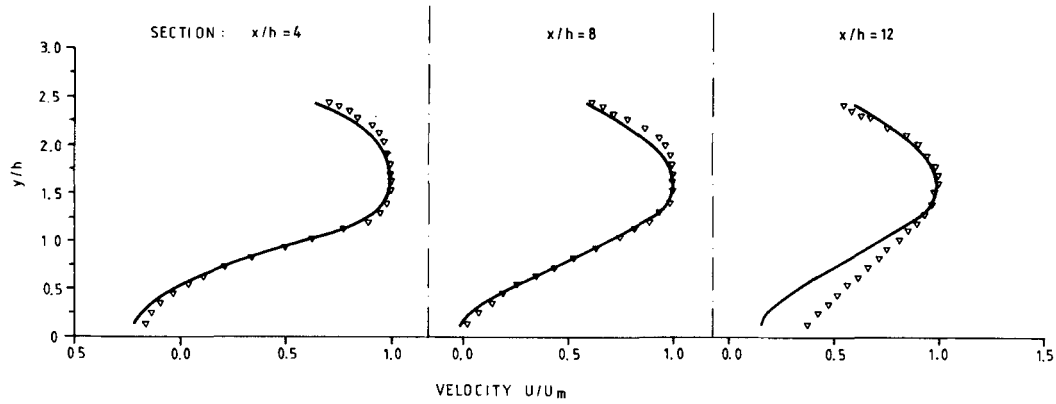

Figure 7. Velocity profiles for backward-facing step problem: ——, present computation; ▽, Westphal *et al.*[25]

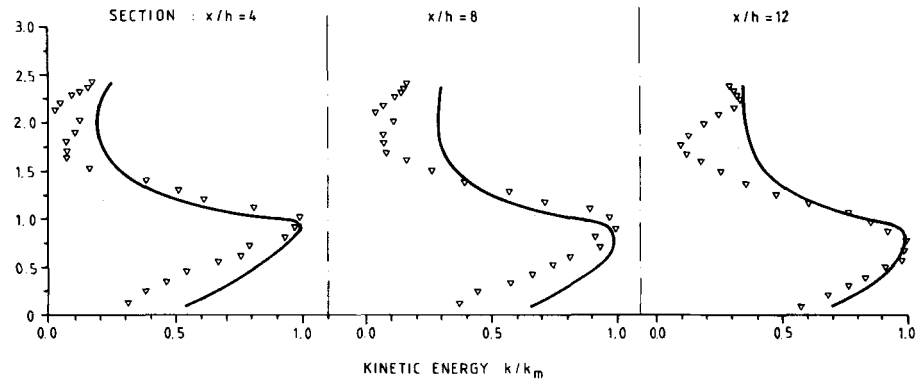

Figure 8. Kinetic energy profiles for backward-facing step problem: ——, present computation; ▽, Westphal *et al.*[25]

been shown by Autret *et al.*[11] that modifications of C_μ will have a relatively strong influence on the results. A similar effect was demonstrated by Smith[8,9] by changing the C_1-value in the ε equation. Preliminary results from the present computations indicate that an increased C_1-value tends to increase the reattachment length. Another problem with the present formulation is the boundary condition applied at the lower wall of the channel. The logarithmic condition is questionable in the recirculation zone and possible inaccuracies here are automatically transferred to the conditions for (k, ε). The latter problem can be solved by using a generalized (k, ε) model,[13] where these equations are solved right down to the wall.

CONCLUDING REMARKS

The aim of this study has been to obtain a robust and flexible computational scheme which is able to handle stationary as well as non-stationary turbulence problems. The computations presented demonstrate the capability of the model to predict the main features of some turbulence problems reasonably well. The solution method was designed to be cost-effective; the algebraic equations are solved by use of a symmetric skyline profile solver and the system is factorized only when

necessary to satisfy the stability requirement. In addition, the complete equation system is solved in a decoupled manner.

Regarding accuracy, the main exception from a conventional FEM discretization is the advection solver. The characteristics method has the desirable quality of being absolute stable, but it should be noted that the Euler scheme applied may imply some numerical diffusion. In this work no direct comparison was made with other numerical methods, except for the 1D time-dependent problem, where results were compared with finite difference computations, showing close agreement.

In this study no special attention has been paid to some of the general problems regarding the limitations of this kind of model, e.g. the boundary conditions in recirculation zones, possible other choices or generalizations of the turbulence model, etc. However, it is believed that some of these problems can be studied by application, modification and generalization of the present model.

ACKNOWLEDGEMENT

I am grateful to Professor G. Moe, the Norwegian Institute of Technology (NTH), for many helpful comments and suggestions during the preparation of this paper.

REFERENCES

1. O. C. Zienkiewicz, R. Loehner, K. Morgan and S. Nakazawa, 'Finite elements in fluid mechanics—a decade of progress', in R. H. Gallaghar *et al.* (eds), *Finite Elements in Fluids, Vol. 5*, Wiley, 1984, pp. 1–27.
2. D. R. Schamber and B. E. Larlock, 'Computational aspects of modeling turbulent flows by finite elements', in K. Morgan *et al.* (eds), *Computer Methods in Fluids*, Pentech Press, 1980.
3. C. Taylor, C. E. Thomas and K. Morgan, 'Analysis of turbulent flow with separation using the finite element method', in C. Taylor and K. Morgan (eds), *Computational Techniques in Transient and Turbulent Flow*, Pineridge Press, 1981.
4. M. J. Soliman and A. J. Baker, 'Accuracy and convergence of a finite element algorithm for turbulent boundary layer flow', *Comput. Methods Appl. Mech. Eng.*, **28,** 81–102 (1981).
5. A. G. Hutton and R. M. Smith, 'On the finite element simulation of incompressible turbulent flow in general two-dimensional geometries', in C. Taylor and B. A. Schrefler (eds), *Numerical Methods in Laminar and Turbulent Flow*, Pineridge Press, 1981.
6. C. Taylor, 'Solving turbulent flow problems using the FEM', in *Finite Elements in Water Resources*, Springer, 1982.
7. A. G. Hutton and R. M. Smith, 'A study of two-equation turbulence models for axi-symmetric recirculating flow', in *Numerical Methods in Laminar and Turbulent Flow*, Pineridge Press, 1983.
8. R. M. Smith, 'On the finite-element calculation of turbulent flow using the k–ε model', *Int. j. numer. methods fluids*, **4,** 303–319 (1984).
9. R. M. Smith, 'A practical method of two-equation turbulence modelling using finite elements', *Int. j. nuber. methods fluids*, **4,** 321–336 (1984).
10. A. G. Hutton, 'Current progress in the simulation of turbulent incompressible flow by finite element method', in *Proc. 4th Int. Conf. on Numerical Methods in Laminar and Turbulent Flow*, Pineridge Press, 1985.
11. A. Autret, M. Grandotto and I. Dekeyser, 'Finite element computation of a turbulent flow over a two-dimensional backward-facing step', *Int. j. numer. methods fluids*, **7,** 89–102 (1987).
12. W. Rodi, 'Turbulence models and their application in hydraulics', *IAHR State-of-the-Art Paper*, Delft, 1980.
13. V. C. Patel, W. Rodi and G. Scheuerer, 'Turbulence models for near-walls and low Reynolds number flows: a review', *AIAA J.* **23**(9), 1308–1319 (1984).
14. J. Douglas and T. F. Russel, 'Numerical methods for convection-dominated diffusion problems based on combining the method of characteristics with finite element or finite difference procedures', *SIAM J. Numer. Anal.*, **19,** 5 (1982).
15. M. Bercovier, O. Pironneau and V. Sastri, 'Finite elements and characteristics for some parabolic–hyperbolic problems', *Appl. Math. Modelling*, **7,** 89–96, April (1983).
16. J. P. Benque, B. Ibler, A. Keramsi and Labadie, 'A finite element method for Navier–Stokes equations', in *Proc Third Int. Conf. on Finite Elements in Flow Problems*, Banff, Alberta, Univ. Calgary, Dep. Mech. Eng. 1980.
17. J. M. Hervouet 'Application de la métode des charactéristiques en formulation faible á la résolution des équations d'advection bidimensionell sur des maillages grilles', *Rapport E.D.F. (Electricité de France), E41/84.11*, 1984.
18. A. M. Baptista, E. E. Adams and K. D. Stolzenbach, 'The 2-D, unsteady, transport equation solved by the combined use of the finite element method and the method of characteristics', in *Finite Elements in Water Resources*, 1984, Springer, pp. 353–362.

19. M. S. Engelman, R. L. Sani, P. M. Gresho and M. Bercovier, 'Consistent versus reduced integration penalty methods for incompressible media using old and new elements', *Int. j. numer methods fluids*, **2**, 25–42 (1982).
20. J. N. Reddy, 'On penalty function methods in the finite element analysis of flow problems', *Int. j. numer. methods fluids*, **2**, 151–171 (1982).
21. S. V. Patankar, *Numerical Heat Transfer and Fluid Flow*, Hemisphere, Washington, DC, 1980.
22. G. D. Tong, 'A treatment of wall boundaries for (k–ε) turbulence modelling within an integral (finite element) formulation', in *Proc. Fourth Int. Symp. on Finite Element Methods in Flow Problems*, North-Holland Publ. Co. 1982.
23. J. Laufer, 'Investigation of turbulent flow in a two-dimensional channel', *NACA Report No. 1053*, 1951, pp. 1247–1266.
24. I. G. Jonsson and N. A. Carlsen, 'Experimental and theoretical investigations in an oscillatory turbulent boundary layer', *J. Hydraul. Res.*, **14**, 45–60 (1976).
25. R. V. Westphal, J. P. Johnston and J. K. Eaton, 'ExperimentaL study of flow reattachment in a single-sided sudden expansion', *NASA Contractor Report 3765—Report MD-41*, Stanford University, 1984.
26. F. Durst and C. Tropea, 'Flow over two-dimensional backward-facing steps', in *Structure of Complex Turbulent Shear Flow*, Springer, 1983.
27. U. K. Kaul and D. Kwak, 'Computation of internal turbulent flow with a large separated flow region', *Int. j. numer methods fluids*, **6**, 927–937 (1986).